JOURNAL OF GEOPHYSICAL RESEARCH, VOL. 105, NO. D16, PAGES 20,473–20,486, AUGUST 27, 2000

Variability-lifetime relationship for organic trace gases: A novel aid to compound identification and estimation of HO concentrations

J. Williams, H. Fischer, G. W. Harris,[1] P. J. Crutzen, and P. Hoor
Max Planck Institute for Chemistry, Mainz, Germany

A. Hansel, R. Holzinger,[2] C. Warneke,[3] and W. Lindinger
Institute for Ionphysics, Innsbruck University, Innsbruck, Austria

B. Scheeren and J. Lelieveld
Institute for Marine and Atmospheric Research, Utrecht University, Utrecht, Netherlands

Abstract. In this study we report aircraft-borne measurements of organic species made during March 1998 in Surinam, an unpolluted region on the northeast coast of South America Measurements included the following: CO by tunable diode laser; a wide variety of organics including acetone, acetonitrile, and isoprene by proton transfer mass spectrometry (PTR-MS); and nonmethane hydrocarbon measurements by gas chromatography-flame ionization detection. Here we compare the standard deviation of the natural logarithm of the mixing ratio (Sigma_lnX) to the estimated lifetime of these species. This relationship has been used to support identification of masses measured by the PTR-MS; ascertain the consistency and quality of hydrocarbon measurement data; and to provide information concerning sinks of important trace species. A selection of the data is used to indirectly determine an average HO concentration of 2.0×10^5 molecules cm^{-3} along the back trajectory for air encountered during the Large-Scale Biosphere-Atmosphere Experiment in Amazonia-Cooperative LBA Airborne Regional Experiment (LBA-CLAIRE) measurement campaign between 0–1 km over the tropical rain forest. The lower than expected HO concentration derived could have been caused by significant atmospheric or oceanic photochemical production of acetone and MEK along the back trajectory.

1. Introduction

The northeast of South America, including Surinam (2.5°–6°N, 54°–57°W) is a very favorable region to study the effects of tropical forest emissions on atmospheric chemistry (see Plate 1). Maritime air masses, depleted in forest hydrocarbons, enter the region with the NNE trades at wind speeds of 5–10 m s^{-1} toward the Intertropical Convergence Zone (ITCZ), which during March was mostly located south of Surinam between 2°S and 1°N. South of 5.5°N the country is almost entirely covered by rain forest (see Plate 1). During the passage of the air over the forests, primary organic emissions and their oxidation products accumulate in the boundary layer.

Here we present measurements of organic species made over the tropical vegetation in Surinam which forms the northern part of the Amazon rain forest. The measurements described were obtained with three independent instruments: a tunable diode laser (TDL); a proton transfer mass spectrometer (PTR-MS), and a gas chromatograph equipped with a flame ionization detector (GC-FID). The TDL made measurements of CO at 1 Hz frequency. The PTR-MS provided measurements of approximately 10 selected gases every 12–20 s (see experimental section), and the GC-FID system was used to analyse the 10 pressurized canisters collected per flight for nonmethane hydrocarbons (NMHCs).

The instruments were flown on a Cessna-Citation II twin-jet aircraft capable of covering the entire country of Surinam. Ten flights of approximately 3.5 hours duration were made during the campaign. Detailed studies of the spatial and temporal distribution of acetone, isoprene, and other trace species detected during Large-Scale Biosphere-Atmosphere Experiment in Amazonia-Cooperative LBA Airborne Regional Experiment (LBA-CLAIRE) campaign have been reported by *Pöschl et al.* [2000], *Warneke et al.* [2000], and *Williams et al.* [2000, also Influence of the tropical rain forest on atmospheric CO and CO_2 as measured by aircraft over Surinam, South America, submitted to *Chemosphere*, 2000, hereinafter referred to as Williams et al., submitted manuscript, 2000]. Here we exploit the high sampling frequency of the PTR-MS and TDL instruments in concert with the highly specific measurements of the GC-FID to study the relationship between variability and lifetime in the rain forest boundary layer. As has been previously reported, variability-lifetime plots can be used to assess data set quality, the presence of halogen radicals, and the remote-

[1]Now at Centre for Atmospheric Chemistry, York University, Toronto, Ontario, Canada.
[2]Now at Max Planck Institute for Chemistry, Mainz, Germany.
[3]Now at Institute for Marine and Atmospheric Research, Utrecht University, Utrecht, Netherlands.

Paper number 2000JD900203.
0148-0227/00/2000JD900203$09.00

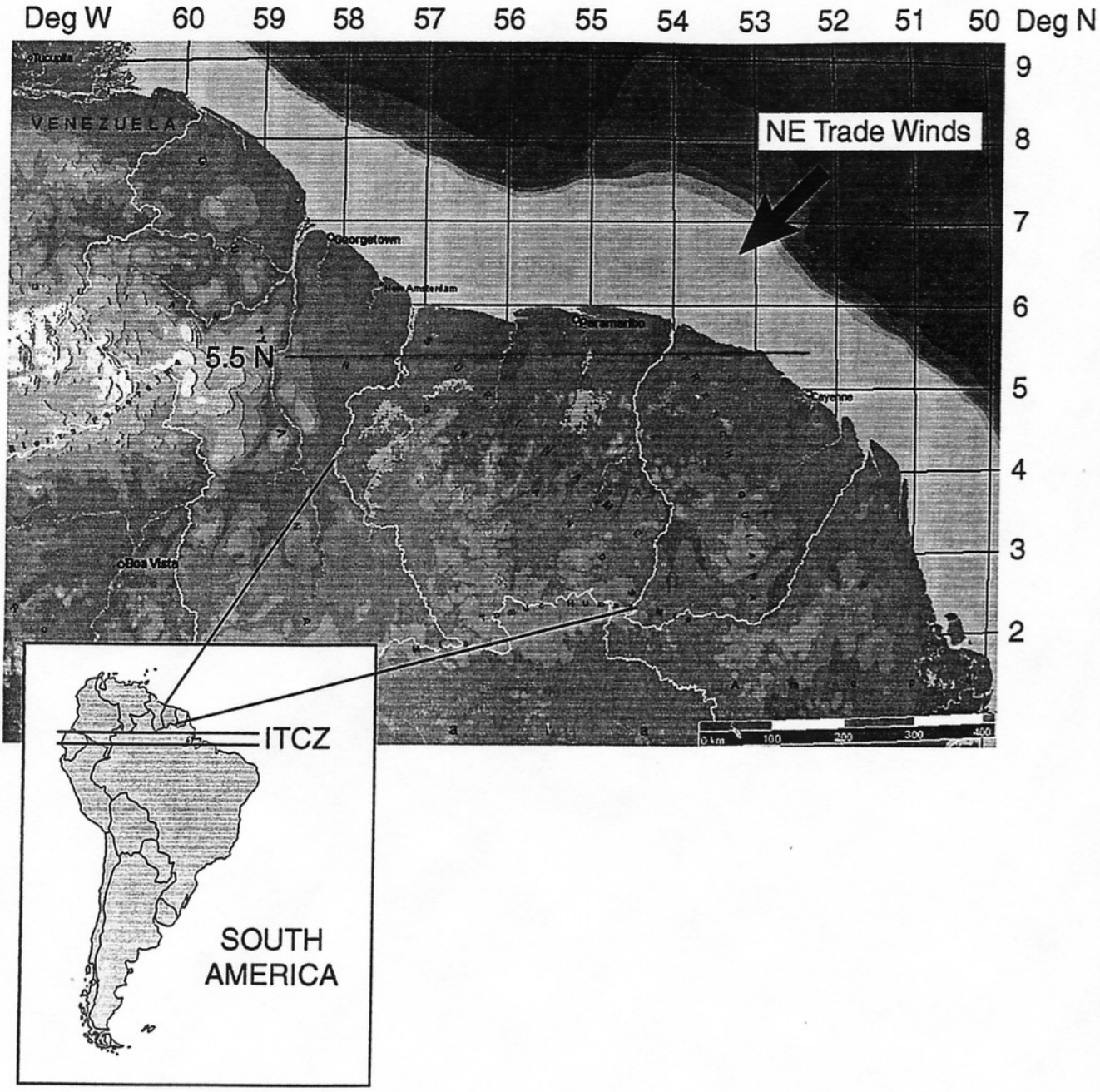

Plate 1. Map of the campaign location. Areas south of 5.5°N are almost entirely rain forest, whereas to the north on the coast there are several small towns and mangrove swamp. The prevailing wind from the surface to 2.5 km was northeasterly, toward the ITCZ.

ness of the measurement location [*Jobson et al.*, 1994, 1998, 1999]. Here we extend the utility of such a treatment to provide supporting evidence for the identification of mass signals from the PTR-MS and to develop a new method for deriving the average HO concentration of the sampled air, along its back trajectory since encountering a source.

2. Experimental Methods

2.1. PTR-MS

The proton transfer mass spectrometer (PTR-MS) has already been used in a variety of ground-based applications [*Jordan et al.*, 1995; *Lindinger and Hansel*, 1997; *Taucher et al.*, 1996; *Warneke et al.*, 1996] and has been described in detail elsewhere [*Lindinger et al.*, 1998; *Hansel et al.*, 1995]. The instrument allows simultaneous, high-frequency measurements of all gases with proton affinities larger than that of H_2O, 166.5 kcal/mol^{-1}. An aircraft version of this instrument was flown for the first time in March 1998 as part of the LBA/CLAIRE field campaign.

Since the PTR-MS does not detect compounds with a proton affinity below 166.5 kcal mol^{-1}, interferences by the major atmospheric constituents N_2, O_2, Ar, and CO_2 are excluded. The exoergicities between H_3O^+ and trace components in the PTR-MS instrument are rather small compared to other ionisation techniques; hence the protonation does not generally

cause the molecule to fragment so that most of the trace species analysed are detected at one mass unit greater than the molecular mass, thus facilitating identification [*Williams et al.*, 2000]. A great advantage of the PTR-MS is that it allows simultaneous, high-frequency measurements; however, a disadvantage of the PTR-MS system is that several ambient gases can contribute to the same mass. For example, the isoprene degradation products methyl vinyl ketone and methacrolein produce a signal at mass 71. Also, the structural isomers propanone (acetone) and propanal (propaldehyde), and glyoxal are indistinguishable from each other by this technique as they are all detected at mass 59 after protonation. In the laboratory a number of techniques have been employed to distinguish between ionic components of the same mass [*Hansel et al.*, 1995]. Varying the drift tube electric field can specifically identify water clusters from certain ions; a consideration of isotopic abundances can on occasion allow structural deduction; and H_3O^+ pulsing can in some cases distinguish between species by differential detection times. Such techniques are, however, not practicable in an airborne experiment where aircraft time is limited and where the spatial variability of compounds is high. In this case the major contributors to a given mass must be elucidated through comparison with results obtained with other techniques in similar environments, knowledge about expected intermediates in the major oxidation processes, model simulations, observed variations with altitude, and dependence on time of day and travel time from the Atlantic coast. It was in most cases possible to identify likely candidates for the mass peaks measured [*Williams et al.*, 2000]. The data treatment described below gives supporting evidence to the mass identification as described below.

Optimization of the PTR-MS technique for airborne measurement resulted in detection limits for most species of approximately 300 pmol/mol (1 pmol/mol is 1 parts per trillion by volume (pptv) in U.S. units). While airborne, the PTR-MS measured a small number of selected masses (about 10 masses for every 12–20 s). The statistical scatter of the data is typically ±10% at volume mixing ratios larger than 5 nmol/mol and ±30% at 1 nmol/mol (1 nmol/mol is 1 ppbv in U.S. units). The errors in the absolute values are within 30%.

In the present study we use PTR-MS measurements of mass 33 (methanol, CH_3OH), mass 42 (acetonitrile, CH_3CN), mass 45 (acetaldehyde, CH_3CHO), mass 59 (acetone, CH_3COCH_3), mass 63 (dimethylsulfide, CH_3SCH_3), mass 69 (isoprene, C_5H_8), mass 71 (methacrolein/methyl vinyl ketone, C_4H_7O), mass 73 (methyl ethyl ketone, $CH_3CH_3COCH_3$), and mass 75 (hydroxyacetone, CH_3COCH_2OH). A detailed explanantion for the identification of these mass signals in this experiment is given by [*Williams et al.*, 2000].

2.2. TDL

A tunable diode laser absorption spectrometer (TDLAS) was used to determine ambient CO mixing ratios. The system applied was specifically designed for airborne trace gas measurements. CO was detected with an integration period of 1 s with a precision of ±2% (1σ) and a calibration accuracy of 2.8% during the 10 measurement flights performed during the LBA-CLAIRE campaign. The instrument design has been described in detail elsewhere [*Wienhold et al.*, 1998].

2.3. GC-FID

Air samples are collected in electropolished stainless steel canisters (manufactured by the Max Planck Institute for Chemistry). In flight the canisters are flushed for 1 min before being pressurized to 3 atm by means of a stainless steel metal bellows pump. The sampling system has been described elsewhere [*Lelieveld et al.*, 1999] and therefore is only briefly summarized below. The air samples were analyzed for C_2-C_7 hydrocarbons using a HP 6890 gas chromatograph fitted with a flame ionization detector. Separation was effected using a 50 m × 0.32 mm Silica porous layer open tubular (PLOT) column, Al_2O_3/KCl, (Chrompack; 60 m × 0.53 mm). 1000 mL samples were preconcentrated in a cryogenic trap prior to injection. The total uncertainty was defined as the sum of the precision of the analysis and the absolute accuracy of the calibration gas, as certified by the supplier. The accuracy for the NMHC standard gas is 3%. Detection limit of the analysis is 15 pmol/mol for all compounds. The precisions for compounds above 15 pmol/mol are as follows: for ethane, 4%; acetylene, 11%; propane, 5%; i-butane, 15%; n-butane, 7%; i-pentane, 25%; n-pentane, 9%; benzene, 6%; toluene, 7%.

3. Results

A preliminary assessment of the data sets generated from each instrument during the LBA-CLAIRE campaign was made using a cumulative Gaussian distribution plot. Examples of such plots are shown in Figure 1 for CO, acetone, ethane, i-pentane, benzene, and methanol. A straight line on this slope indicates that the data have a Gaussian distribution. However, both measurements and instrumental noise can have such a distribution. Deviations from the straight line are expected in the case of stochastic events exemplified by the CO and benzene plots whose highest concentrations are associated with the crossing of a high-altitude biomass burning plume (Williams et al., submitted manuscript, 2000). An unusual distribution is also observed when analytical errors such as chromatographic peak splitting occasionally occur. The whole peak is not always integrated (e.g., ethane); and the distribution then appears divided into two distinct sections. Moreover, when the chromatographic peaks integrated are below the detection limit of the system, then integration of the background at that retention time repeatedly yields the same value distorting the plot, for example, i-pentane. Despite identification of the aforementioned measurement problems with some elements of the data set, we have used the data as given in the following study and highlight how variability lifetime relationships for a campaign data set can be used to highlight the erroneous data as well aiding identification of masses by the PTR-MS and derive semiempirical HO concentrations.

3.1. Variability

For a large measurement data set we can assess the variability of a species by examining the standard deviation of the measurement. The mixing ratios measured and the calculated variability in a given region can be understood in terms of the source sink paradigm. Intuitively, we expect to observe most variability from species that are most rapidly removed from the atmosphere, whose inhomogeneous sources are nearby or whose sources vary greatly with time. The overall rate of removal of species from the atmosphere is dependent on the chemical nature of the species, and may include contributions from the reaction with HO radicals, photolysis, and heterogeneous processes. This concept was first explored for the global distribution of long-lived atmospheric species by *Junge* [1974], who determined that the relative standard deviation (standard

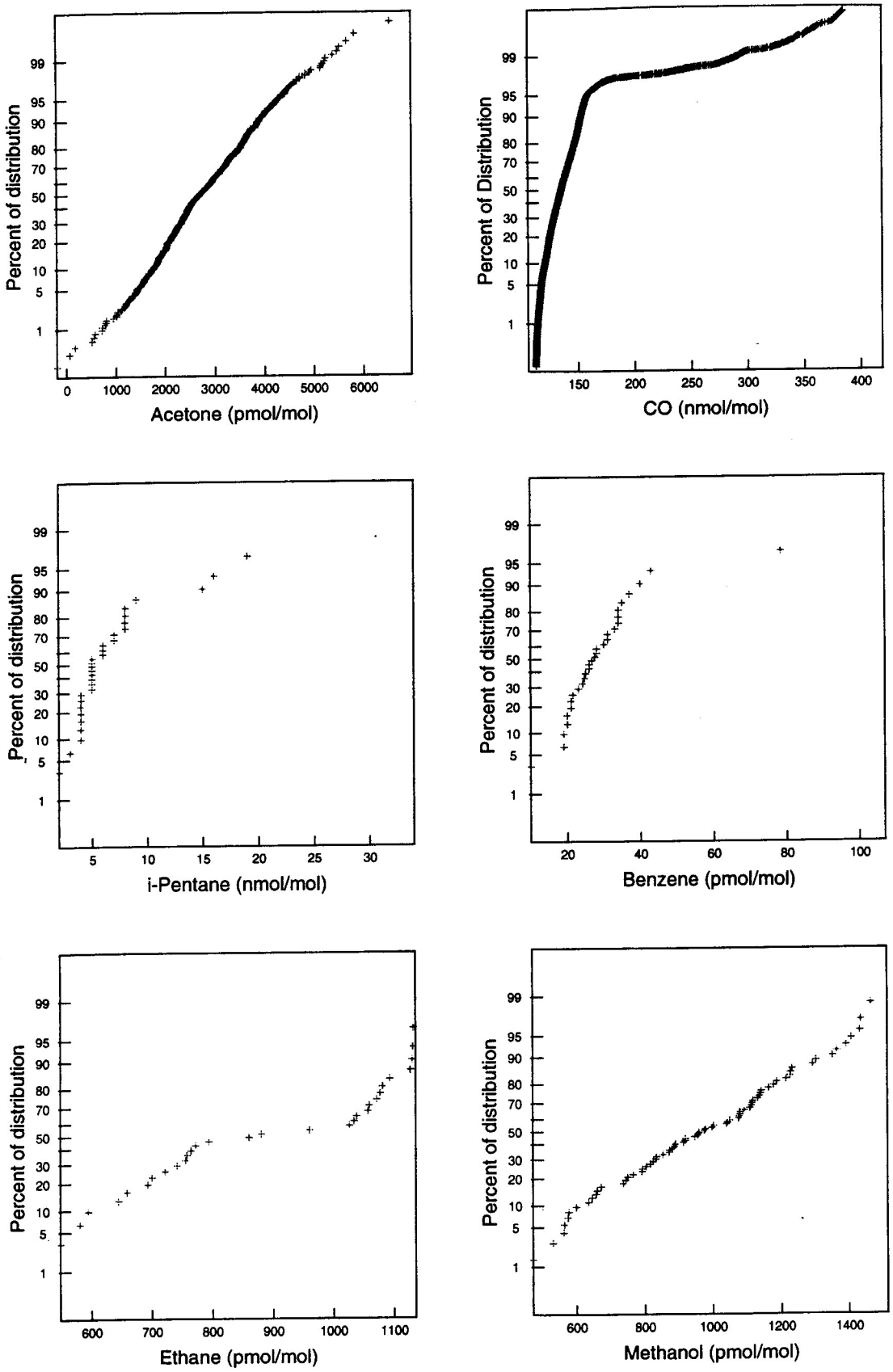

Figure 1. The cumulative Gaussian distribution plots for acetone, CO, benzene, i-pentane, ethane, and methanol for the LBA-CLAIRE campaign are shown.

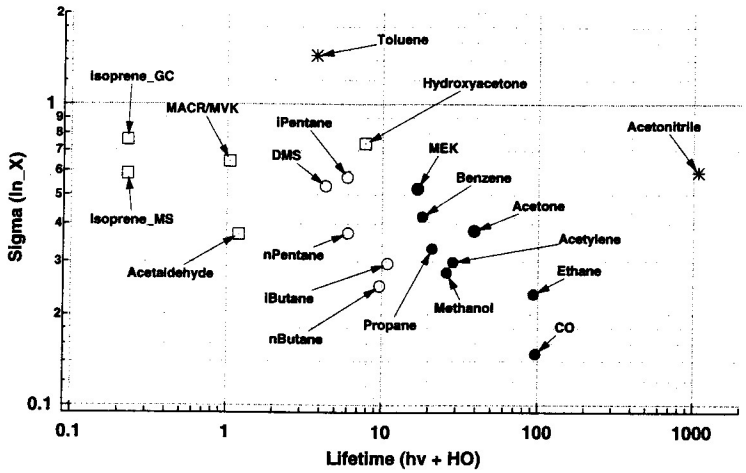

Figure 2. Sigma_ln(X) against lifetime in days for 20 species. Only data between 0–1 km in altitude and south of 5.5°N latitude are included. CO was measured by tunable diode laser. Ethane, propane, acetylene, i-butane, n-butane, i-pentane, n-butane, benzene, and toluene were measured by GC-FID, and all other species presented were determined by the PTR-MS. Acetone and MEK are highlighted with a cross.

deviation divided by the mean concentration) was inversely proportional to the residence time in years. This inverse dependency on lifetime has been reproduced in model studies by *Hamrud* [1983], who concluded that the spatial relation between sources and sinks strongly influences trace gas spatial variability, with the τ^{-1} dependency only being approached for very long-lived species. *Jobson et al.* [1998] extended studies of the variability-lifetime relationship to nonmethane hydrocarbons on a regional scale. They report empirical relationships between the measured variability and the HO lifetime for hydrocarbons and halocarbons for a wide range of data sets [*Jobson et al.*, 1999, 1998]. The aforementioned works introduce the standard deviation in the natural logarithm of the mixing ratio, Sigma_ln(X), as a more tractable assessment of variability for short-lived gases. This relationship was given as

$$\text{Sigma\_ln(X)} = A\tau^{-b}$$

where τ is the lifetime and A is a fitting parameter determined in the regression. The exponent b has a value between 0 and 1, being an indicator of the relative strength of sink terms and turbulent mixing upwind of the measurement location. *Jobson et al.* [1999] used Sigma_ln(X) instead of the relative standard deviation to consider the statistics of an exponentially decaying function sampled over a finite period. In the limit of small variability (long chemical lifetimes), Sigma_ln(X) equals the relative standard deviation [*Jobson et al.*, 1998], but at high variability (small chemical lifetimes), Sigma_ln(X) gives much simpler behavior. Recently, *Ehhalt et al.* [1998] used a three-dimensional tracer model to study variability-lifetime relationships. Their conclusions are similar to the results of the studies performed by *Jobson et al.* [1999, 1998]; in particular, they found the dependence on τ to vary with geographical location. Within their model, proximity to continental sources produced a weaker τ dependence than remote oceanic environments. On a regional basis their model predicts a much weaker lifetime dependency than the inverse relationship predicted by *Junge* [1974]. In general, examination of derived trends for variability-lifetime relationships provides insights into the hydrocarbon data set quality, the remoteness of the location from sources, and into general atmospheric processing.

A plot of Sigma_ln(X) against lifetime for 20 species measured during the LBA-CLAIRE campaign is shown in Figure 2. Only data between 0–1 km in altitude and 1°–5.5°N latitude are included. Areas south of 5.5°N are almost entirely rain forest, whereas to the north on the coast there are a few small towns and mangrove swamp. Air in the "mixed layer" between 0–1 km has been advected from over the Atlantic Ocean by the northeasterly trade winds and is expected to be well mixed and in contact with the forest. All rate data used are given in Table 1. The diurnal average HO concentration used in this plot is 5×10^5 molecules cm^{-3} which is in accordance with estimates made by *Crutzen et al.* [1985]. HO reaction rate coefficients are taken where possible from recommendations of the most recent literature reviews. Photolysis rates were calculated with an updated version of the radiation model of *Brühl and Crutzen* [1989], and one quarter of the noontime maximum value is taken as the diurnal average photolysis rate.

A general trend from highly variable short-lived compounds to less variable long-lived compounds is observable in some of the data. The points corresponding to methyl ethyl ketone, acetone, methanol, benzene, propane, ethane, acetylene, and CO (solid circles) as well as toluene and hydroxyacetone are correlated and show an inverse dependence of variability with lifetime. Showing the same trend but lying away from the line are n-pentane, n-butane, and i-butane (open circles), while acetonitrile (star) does not fit with the general trend at all. Measured compounds with lifetimes under 2 days, isoprene, acetaldehyde, and methacrolein/methyl vinyl ketone (open squares), appear not to fit with the trend and show less variability than would be expected for molecules with such short lifetimes according to the trend in the species denoted with solid circles.

The fact that such a trend can be seen is most interesting. The data are from three separate instruments, for molecules with a variety of chemical characteristics, and are taken over a wide geographical domain. A good fit to this treatment has been suggested as indicative that the sampling site is remote and that the influence of local sources is small [*Jobson et al.*, 1998]. This is clearly not the case over a tropical rain forest where a wide variety of compounds can be emitted [*Kesselmeier*

Table 1. Photolysis and HO Removal Rates Used in This Study

Measured Species	Instrument	HO Reaction Rate,[a] cm^3 molecule s^{-1}		Photolysis Rate,[b] s^{-1}
Mass 33 (methanol)	PTR-MS	8.95×10^{-13}	[*Demore et al.*, 1997]	NA
Mass 42 (acetonitrile)	PTR-MS	2.16×10^{-14}	[*Atkinson et al.*, 1997]	NA
Mass 45 (acetaldehyde)	PTR-MS	1.63×10^{-11}	[*Baulch et al.*, 1982]	6.07×10^{-6}
Mass 59 (acetone)	PTR-MS	1.90×10^{-13}	[*Le Calve et al.*, 1998]	8.01×10^{-7}
Mass 63 (DMS)	PTR-MS	5.37×10^{-12}	[*Turnipseed et al.*, 1996]	NA
Mass 69 (isoprene)	PTR-MS	1.01×10^{-10}	[*Atkinson et al.*, 1986]	NA
Mass 71 (MVK and MACR)[c]	PTR-MS	1.22×10^{-11}	[*Gierczak et al.*, 1997]	3.24×10^{-6}
	PTR-MS	2.76×10^{-11}	[*Gierczak et al.*, 1997]	5.14×10^{-6}
Mass 73 (MEK)	PTR-MS	9.72×10^{-13}	[*Le Calve et al.*, 1998]	8.01×10^{-7} [d]
Mass 75 (hydroxyacetone)	PTR-MS	3.00×10^{-12}	[*Atkinson et al.*, 1997]	NA
Mass 101 (isoprene hydroperoxides)[e]	PTR-MS	9.08×10^{-11}	[*Jenkin et al.*, 1997]	5.76×10^{-6} [f]
Ethane	GC-FID	2.49×10^{-13}	[*Atkinson et al.*, 1997]	NA
Propane	GC-FID	1.11×10^{-12}	[*Atkinson et al.*, 1997]	NA
Acetylene	GC-FID	8.15×10^{-13}	[*Atkinson*, 1989]	NA
n-Butane	GC-FID	2.39×10^{-12}	[*Donahue et al.*, 1998]	NA
i-Butane	GC-FID	2.13×10^{-12}	[*Donahue et al.*, 1998]	NA
n-Pentane	GC-FID	3.85×10^{-12}	[*Donahue et al.*, 1998]	NA
i-Pentane	GC-FID	3.90×10^{-12}	[*Atkinson et al.*, 1986]	NA
Toluene	GC-FID	6.19×10^{-12}	[*Atkinson et al.*, 1986]	NA
Benzene	GC-FID	1.28×10^{-12}	[*Atkinson et al.*, 1986]	NA
CO	TDL	2.40×10^{-13}	[*Demore et al.*, 1997]	NA

NA, not applicable.

[a]All rates used are at 298 K and 1000 mbar, conditions which approximate those of the Surinam boundary layer.

[b]The average noontime photolysis rate between 5°–35°N in March from the photolysis model of *Brühl and Crutzen* [1989]. These data include the effect of clouds which are incorporated into the global photolysis scheme from a standard cloud atlas; tropopause is fixed at 98 mbar. One quarter of these values is taken in this study for the diurnal average photolysis rate.

[c]Photolysis and HO rates were calculated for mass 71 based on the relative product yields by *Tuazon and Atkinson* [1990].

[d]Photolysis rate calculated as acetone.

[e]The rate used is the average of the rates from the four isomers detailed in the Master Chemical Mechanism (MCM).

[f]Photolysis rate calculated as CH_3OOH.

and Staudt, 1999]. The interpretation of these analyses must therefore be reexamined.

A number of the molecules contained within the general trend are for the most part not directly emitted from the rain forest but from remote sources and brought to Surinam via the northeasterly trade winds. These molecules include acetylene, benzene, propane, ethane, and CO. After emission, they are advected toward Surinam and en route are depleted through their reaction with the HO radical, although to a small extent CO is also produced more locally from hydrocarbon photochemical decomposition (Williams et al., submitted manuscript, 2000). As they pass through the measurement domain, defined as 1 km high and from 1° to 5.5°N over Surinam, they are also removed by reaction with HO. Transport through the measurement domain takes approximately 1 day. The variability observed in the mixing ratios of the aforementioned species, determined throughout the measurement domain, is inversely related to lifetime. This behavior indicates that the measurement domain is remote from the sources of these species according to the interpretation of *Jobson et al.* [1998]. However, also within this trend are the molecules acetone, methyl ethyl ketone, methanol, and hydroxyacetone. Acetone is emitted from living and decaying plant matter [*Kirstine et al.*, 1998; *Warneke et al.*, 1999], methyl ethyl ketone has been reported from living and freshly cut grass [*Kirstine et al.*, 1998; *de Gouw et al.*, 1999], methanol is emitted from decaying biomass [*Warneke et al.*, 1999], and hydroxyacetone is a photooxidation product of isoprene.

The molecules n-butane, i-butane, n-pentane, i-pentane, and dimethyl sulfide (DMS) appear to show a similar but offset trend to that discussed above. A closer examination of the alkane data, using a Gaussian cumulative distribution plot, shown in Figure 1, revealed in each case a high incidence of certain mixing ratios, indicating that the instrument was operating close to or at its detection limit. We conclude that for these four species the chromatographic peak integration was being performed on the instrument background. The background signal shows little variability, and the small concentrations repeatedly calculated from background integration serve to suppress the apparent variability of these species. The reason why the pentanes and butanes all lie on a parallel trend with a seemingly constant offset is that the sources of these compounds are highly correlated and approximately the same fraction of these compounds lie below the detection limit of the GC system. The variability is therefore "artificially" reduced by the same amount. Although toluene lies on general trend, closer inspection of the data provided show this to be merely coincidental. The toluene peak in the GC analysis is well resolved, and no evidence of a neighboring interferrent peak has been noted. However, a small number of elevated values of toluene were found to give rise to the high variability. These are not correlated with increases in other hydrocarbons. Toluene has been recently reported as an emission from certain plant species, most strongly when plant wounding has occurred [*Heiden et al.*, 1999]. To induce such variability in the measurements, emission would have to be restricted to certain areas. Observers on board the aircraft reported only homogenous rain forest in the regions flown. It is therefore concluded

Table 2. Relative Contribution to Variability Compared to Instrumental Precision for Nine Equispaced Sources

Source Number	Cumulative Fraction	Percent Precision to Detect Source	Instrument Precision Limits, %	4-Day Lifetime Time Between Sources	Distance, km Wind Speed 5 m s^{-1} 4-Day Lifetime	Distance, km Wind Speed 5 m s^{-1} 40-Day Lifetime	Distance, km Wind Speed 5 m s^{-1} 2-Day Lifetime
1	0.6321	36.9		4	1,728	17,280	432
2	0.8646	13.5		8	3,456	34,560	864
3	0.9502	4.98	5	12	5,184	51,840	1,296
4	0.9817	1.83		16	6,912	69,120	1,728
5	0.9933	0.67	1	20	8,640	86,400	2,160
6	0.9975	0.25		24	10,368	103,680	2,592
7	0.9991	0.09	0.1	28	12,096	120,960	3,024
8	0.9997	0.03		32	13,824	138,240	3,456
9	0.9999	0.01	0.01	36	15,552 continental	155,520 global	3,888 regional

Assuming a constant 5 m s^{-1} wind shows species with 2, 4, and 40 day lifetimes to be influenced by sources on a regional, continental, and global scale.

that the high concentrations of toluene measured in four canisters, which give rise to the high variability, result from a system artifact or contamination rather than a genuine atmospheric process. When the suspect canisters are removed from the study, the calculated variability falls well below the general trend as many of the measurements lie below the detection limit and quantized mixing ratios, similar to the butanes and pentanes, are seen in the data. The presence of toluene within the trend was due to the effects of variability enhancement due to contamination and variability suppression due to values below the detection limit cancelling out. Chromatographic problems were also found for ethane which was found to be an outlier above the general trend when used to derive HO concentrations by the method described below. Occasional splitting of the ethane peak, possibly caused by the absence of a CO_2 trap in the system, and incorrect integration artificially enhanced the measured variability. Such cases show the utility of this data treatment as a quality check on hydrocarbon data sets, a technique that was first exploited by *Jobson et al.* [1998]. Owing to these measurement problems, the toluene and ethane data were not used in this study.

Deviation of DMS from the trend cannot be explained in the same way as the outlying alkanes. However, in the case of DMS, the lifetime of the species in this study may have been overestimated as the reaction of ozone has not been included. This would reduce the lifetime and may cause DMS to behave similarly to the short-lived compounds isoprene, acetaldehyde, and MACR + MVK which all lie below the trend line. In this study the molecules with lifetimes less than 2 days show a variability which is less than that expected by the general trend. A suppressed variability for species with lifetimes less than 5 days has also been reported for compounds measured in canisters [*Jobson et al.*, 1998].

We can understand this observation by considering simple models for the variability concept. The first is simply a source and a point of measurement. Emissions from the continually emitting source can take a variety of travel times to reach the point of measurement, each of which will result in differing extents of chemical depletion. Assuming that the compounds decay exponentially after being emitted and provided that the mixing ratio of the chemical species in question does not reduce to below the instrument detection limit, and that the source is not so proximate as to prevent a range of air ages being sampled, then the variability of the species at the point of measurement will be inversely proportional to the lifetime. We now consider the case of a line of sources each continuously emitting a species, and a detector some distance from but in line with the sources. Assuming a constant wind along the sources and a distance equivalent to one lifetime of the species between each source, the cumulative contribution to the measured concentration is given for each source in Table 2. From this cumulative contribution the instrumental precision required for detection of the contribution emitted from each source can be calculated. Assuming an instrumental precision of 1%, then we calculate that the variability is sensitive to sources distant up to between 4 and 5 lifetimes of the species (see Table 2). For a species with a lifetime of 4 days (e.g., pentane) and assuming a constant 5 m s^{-1} wind speed, then we estimate that the variability of this species can be affected by sources over 7000 km distant from the detector, equivalent to the size of a continent. For species with longer lifetimes the distance equivalent to 5 lifetimes encompasses the entire globe meaning that the variability of such species can, theoretically, be affected by all sources within the hemisphere. Measurements of short-lived species can be influenced only by sources within a much smaller domain. The variability of different molecules therefore can be affected by sources at different distances back along the back trajectory. When several molecules of different lifetimes stem from the same distant source, we expect their variability to be inversely dependent on the lifetime through the coefficient b which relates the relative influence of chemistry and dynamics. However, if the lifetime of the molecule is short enough, distant sources do not influence the variability above the instrumental precision, and this species cannot be expected to lie in the same trend with the same A coefficient.

Strong nearby sources can strongly affect the calculated variability. This may destroy any correlation between Sigma_ln_X and lifetime, as has been shown by *Jobson et al.* [1998]. Reexamining Figure 1, we note that hydroxyacetone, a photoproduct of isoprene, can be associated with both isoprene and MACR/MVK, and this group appears to show no real correlation between variability and lifetime. As described above, this is expected for species with strong local sources. The trend in isoprene and products is complicated by the strong diurnal cycle in isoprene emission which also induces variability in the measurements. Therefore the presence of hydroxyacetone in the trend of species such as benzene and propane may be either coincidence of two intersecting trend lines or an indication that the remote source dominates over the local biogenic

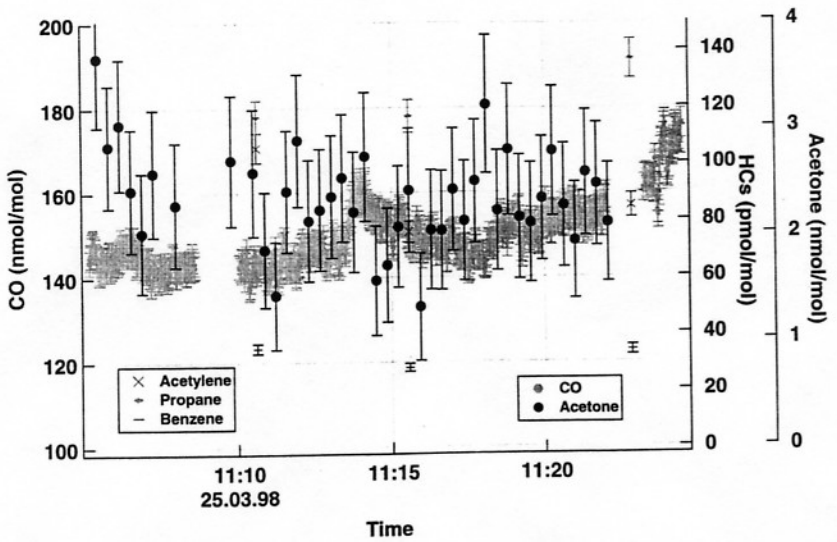

Figure 3. The change in mixing ratio as a function of time for several species measured by TDL (CO), GC-FID (acetylene, propane, benzene), and PTR-MS (acetone). In all cases the atmospheric variability observed is greater than the (1 sigma) error bars shown. The variability is determined by atmospheric processes and not by the instrument precision.

source. The former seems more probable as the ambient mixing ratios of its precursor isoprene over the rain forest were high, up to 8 nmol/mol (ppbv in U.S. units) and variable diurnally [*Warneke et al.*, 2000]. Acetone, MEK, and methanol lie on the trend with benzene, propane, and acetylene which is consistent with the expectation that they originate from distant source regions and that isoprene oxidation (or other strongly varying local emission) is not the dominant source of these species. In the case of acetone the mixing ratios measured over the rain forest were between 1–2 nmol/mol [*Pöschl et al.*, 2000], so acetone over continental sources would have to be much higher to dominate the biogenic emissions. High mixing ratios of acetone have been reported: 10–40 nmol/mol from the metropolitan area of Denver, Colorado [*Anderson et al.*, 1996], 1–18 nmol/mol from the Fraser valley [*O'Brien et al.*, 1997], and even higher could be expected from industrialized Europe. Another possibility is that the sources of acetone, methanol, and MEK over the forest are relatively constant with time and spatially homogeneous and therefore do not affect the measured variability significantly. For this explanation to be true, the sources of these compounds cannot exhibit a diurnal cycle similar to isoprene but may be similar to terpenes, emission of which depends on temperature but not on light and hence does not vary greatly throughout the day in tropical regions.

The variability of the acetonitrile measurement is much greater than would be predicted from the trend for a compound with a 3 year lifetime. Four possible explanations for this deviation from the trend have been considered: The first is measurement error, for example, the mass may correspond to another molecule more reactive than acetonitrile; second, nearby scattered sources such as fires may have induced an abnormal variability; third, the rain forest is a strong or varying source of acetonitrile; or fourth, the atmospheric lifetime of this molecule is overestimated. The potential for an interferent molecule at this mass is small. As the molecular mass is low, the number of potential interferent organic molecules is limited. Furthermore, as molecules containing exclusively carbon, hydrogen, and oxygen always have an even molecular mass, molecules detected at protonated mass 42 must include an odd valent atom such as nitrogen [*Williams et al.*, 2000]. Acetonitrile can also be produced from biomass burning [*Holzinger et al.*, 1999], and the presence of scattered fires in the region would lead to greater variability in the measurement. This, however, can be discounted as such burning events would also give rise to CO and the point corresponding to CO follows the general trend. There are no reported measurements of acetonitrile as a biogenic emission. Therefore we conclude that the removal rate used in Figure 1 for acetonitrile is not correct. Assuming that the HO reaction rate with acetonitrile is correctly determined, then a second removal process must be important. Photolysis of acetonitrile can be discounted as it does not appreciably absorb in the actinic region. Although Henry's law coefficients for acetonitrile are not high (5.3×10^2 M/atm) [*Benkelberg et al.*, 1995], a residence time of 15 days was calculated for ocean uptake when reverse flow was neglected [*Hamm et al.*, 1984]. While the rate of hydrolysis of acetonitrile in alkaline solution is slow [*Wideqvist*, 1956], conditions over the rain forest will be more acidic [*Andreae et al.*, 1988], and wet surfaces may contain other species that can react with acetonitrile such as alcohols. If a lifetime of 15 days is used, then the acetonitrile point fits the general trend observed in the other data. The presence of such an uptake may be an important component of the nitrogen budget of the forest, particularly in the burning season when high concentrations of acetonitrile can be expected. Moreover, the global source, currently estimated at 1.6 Tg yr^{-1} [*Schneider et al.*, 1997], would have to be scaled up by more than an order of magnitude in order to balance the budget.

The existence of a trend in the variability versus lifetime plot shows that the precision of the instruments concerned is better than the atmospheric variability. This can also be seen from an example of the data used in this treatment, shown in Figure 3. The data shown were all taken below 1 km altitude, and the precision for each measurement is included as an error bar. It can be seen that for CO (TDL), for acetone (PTR-MS), and for propane, acetylene, and benzene (GC-FID) the variations observed in the measurement are in each case greater then the statistical error. It should be noted that provided the data are

above the detection limit of the instrument the calculated variability is independent of the mixing ratios measured. The variability lifetime analysis provides a method to judge whether the precision is greater than the atmospheric variability which is more rigorous than qualitative assessment by eye.

3.2. An Aid in Compound Identification for the PTR-MS

The measurements of the nonmethane hydrocarbons and CO are highly specific, whereas the PTR-MS measures the concentration of molecules of a chosen mass. The identity of the primary contributor to a given mass signal must be deduced by comparison with results obtained with other techniques in similar environments, knowledge about expected intermediates in the isoprene oxidation chain, model simulations, observed variations with altitude, and dependence on time of day and travel time from the Atlantic coast [*Williams et al.*, 2000]. The presence of molecules measured by the PTR-MS in the same trend lends some credence to the identification of the primary contributors to each mass measured by the PTR-MS. A potential interference for the PTR-MS would therefore have to have a proton affinity greater than water, a mass equal to that of the species proposed, and the same atmospheric removal rate. The treatment therefore provides valuable supporting evidence for the identification of species measured by the PTR-MS. Two equally likely candidates for a particular mass with different lifetimes could also be differentiated by this technique. For example, in the case of mass 59, possible contributors to this mass include acetone, propaldehyde, and glyoxal. Both propanal and glyoxal have short atmospheric lifetimes due to rapid reaction with HO and photolysis, respectively. The variability measured at mass 59 lies on the trend defined by the other measured species when it is ascribed to acetone. This provides supporting evidence for the assertion that VMRs at mass 59 are predominantly acetone.

It was noted that the variance of isoprene determined by the GC-FID was greater than the variance from the PTR-MS despite the absolute values being in good agreement. Both values for the variability of isoprene are below that expected from the trend observed in molecules with 10–100 day lifetimes. While the number of PTR-MS measurements of isoprene (n = 747) is much greater than that of the GC-FID (n = 32), there is potential interference in the PTR-MS measurements at the same mass. for example, from furan and from 2-methyl-3-butenol. The lifetimes of both of these molecules are longer than that of isoprene but not sufficiently so as to account for the low variance observed. A strong indication for an interfering species masking the PTR-MS isoprene measurements was found in an intercomparison with the GC measurements. Although *Warneke et al.* [1999, 2000] found a high correlation between the PTR-MS and the GC measurement (r^2 = 0.86), the slope of the linear correlation function deviates from unity and exhibits a large intercept (PTR-MS equal to 0.84 × GC + 688 pmol/mol), indicating a significant offset for the PTR-MS measurements. This offset could be due either to the above mentioned interference on mass 69 or caused by an underestimation of the detection limit of the PTR-MS. A higher detection limit would result in larger scatter at low concentrations, giving rise to a significant intercept in the correlation with the GC measurements. The lower variability of the PTR-MS measurements relative to the GC data would then be the result of a certain percentage of the PTR-MS isoprene data falling below the limit of detection, so that the full dynamic range and hence the variability cannot be quantified.

3.3. Calculation of HO Concentrations

A selection of molecules fitting the general trend in the data was used to analyze further the variability lifetime relationship. Plates 2a and 2b show for various HO concentrations a plot of Sigma_ln(X) against lifetime for the selected species which was limited to those with lifetimes between 3 and 100 days. The data for species with lifetimes less than 2 days, namely, isoprene, MACR/MVK, and acetaldehyde, were not included. The butanes and pentanes were not used as the concentrations measured were at or close to the detection limit, which had the effect of suppressing the observed variability. Toluene, acetonitrile, ethane, and hydroxyacetone were also not included for reasons discussed above.

Plates 2a and 2b show a line of best fit (red) to the data for an HO concentration of 5×10^5 molecules cm^{-3}. If the HO concentration employed is varied, and the lifetimes of the species studied were determined exclusively by HO radicals, then we would expect the points merely to shift along the x axis. However, acetone and methyl ethyl ketone are removed by photolysis and HO. This means that variations in the assumed HO concentration will affect the total lifetimes of acetone and methyl ethyl ketone to differing extents. This will give rise to a different distribution of points and hence a different value of chi squared. The chi squared value indicates the discrepancy between the function and the data and evaluates the correlation of the least squares fit; lower values of chi squared mean a better fit to the data. It is then possible to determine the HO concentration which produces the minimum chi squared. This is therefore an empirically derived HO concentration for the data set and represents an average HO concentration along the back trajectory from the point of measurement to the source. The derivation of HO using the concept of variability was originally reported by *Ehhalt et al.* [1998], who noted that, although unavailable, measurements of radon could be used to obtain HO concentrations. Instead, *Ehhalt et al.* [1998] used the competing removal reactions of ozone and HO with various hydrocarbons, and by assuming a constant ozone concentration, derived an HO concentration which gave a best fit to the data. In this work we have a wider variety of chemical species available for this analysis and are able to exploit the dual photolysis and HO removal rates of acetone and methyl ethyl ketone to determine an optimum HO concentration.

Plate 2a shows the observed change in the gradient and the chi squared for varying HO concentrations from the original estimate of 5×10^5 molecules cm^{-3} by a factor of 10. At HO concentrations of 5×10^6 molecules cm^{-3} the scatter in the data and the chi squared value have markedly increased. When HO concentrations are only 5×10^4 molecules cm^{-3}, the chi squared is also higher. In Plate 2b the HO concentrations are varied by a factor of 2. A gradual decrease in chi squared is observed for HO concentrations of 1×10^6, 5×10^5, and 2.5×10^5 molecules cm^{-3}. Optimizing the fit to the minimum chi squared for all selected species produces an HO concentration of 1.95×10^5 molecules cm^{-3} (see Figure 4a).

The optimal HO concentration is sensitive to the photolysis rate chosen; doubling the rate approximately doubles the calculated HO. The estimation of HO is relatively insensitive to the inclusion of the previously discarded outlier ethane in the data treatment, which reduces the calculated HO slightly to

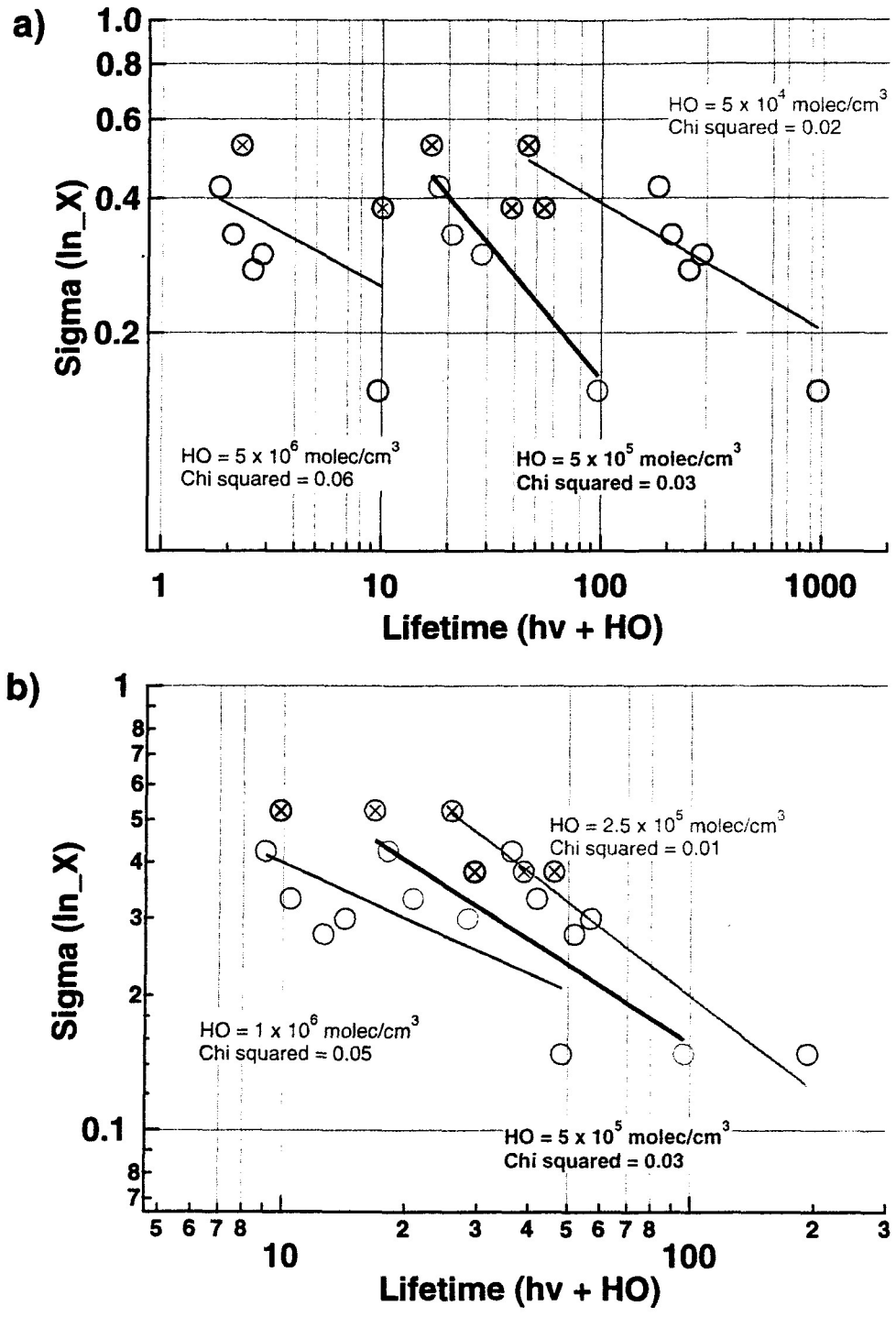

Plate 2. S_ln(X) against lifetime for various HO concentrations for the selected species, limited to those with lifetimes between 3 and 100 days. The red trace in both plots is the fit to Sigma (lnX) = $A\tau^{-b}$ for an HO concentration of 5×10^5 molecules cm^{-3}. Acetone and MEK are highlighted with a cross. HO concentrations varied by (a) a factor of 10 and (b) a factor of 2.

1.75×10^5 molecules cm^{-3}. The coefficients of the fit to the selected species are Sigma_ln(X) equal to 4.63 $\tau^{-0.64}$ (see Figure 4b). The fit is constrained by acetone, MEK, and by the gradient of the other organic species.

The value obtained for HO is interpreted as the average HO encountered along the back trajectory since the source for air masses from 1° to 5.5°N for the campaign duration between March 12 and 29, 1998. From the data selected for the optimization we derive HO concentration 2×10^5 molecules cm^{-3}. This value may be compared with values generated by the Model of Atmospheric Transport and Chemistry-Max Planck Institute for Chemistry (MATCH-MPIC) global model [*Lawrence et al.*, 1999] with improved NMHC chemical parameterization [*Kuhlman et al.*, 1999] for an idealized trajectory extending from Surinam to the northeast over the Atlantic Ocean. The model resolution is 5.6° × 5.6°, and eight grid

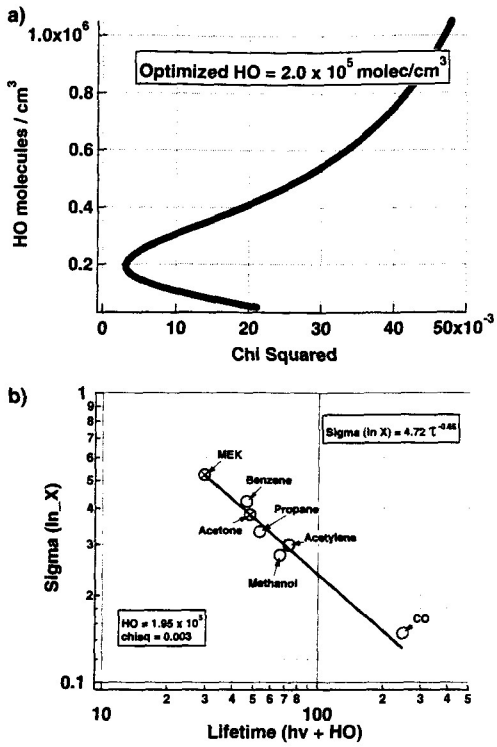

Figure 4. (a) HO concentrations versus chi squared for the data shown in Figure 4b. The effect of the changes in HO on the point distribution can be seen in Plates 2a and 2b. (b) The fit of the selected data from Figure 2 for the optimal HO concentration derived from Figure 4a. Acetone and MEK are highlighted with a cross.

squares lie between Surinam and the coast of Portugal directly to the northeast. The diurnal average HO values in each of these grid squares at 500 m starting with the grid square covering Surinam are 3×10^5, 2.13×10^6, 1.96×10^6, 1.54×10^6, 1.13×10^6, 8.58×10^5, 6.6×10^5, and 5.8×10^5 molecules cm^{-3}, respectively. The value over Surinam is low due to the high ambient mixing ratios of isoprene and low ozone mixing ratios present over the rain forest. Assuming that the wind is indeed consistently northeasterly and hence the source of all the species measured is Europe, we can compare the average of these model averages (1.1×10^6 molecules cm^{-3}) with the estimated HO 2×10^5 molecules cm^{-3} which is the estimated average HO concentration along the back trajectory. It should be noted that no weighting of the HO fields along the trajectory is required in forming the model average for this comparison. The empirically derived HO concentration here is approximately 5 times less than HO predicted by the global model. One reason for the discrepancy is that the air measured did not follow this idealized back trajectory and in reality spent time in the free troposphere where HO concentrations are lower. Another possibility is that the model values are produced from a climatological average meteorology data set for the month of March which may not represent the 2 weeks of measurement in March 1998. For example, large-scale late winter NH weather systems could reduce the HO along the back trajectory below the climatological average. One factor causing the HO concentration to be underestimated could be photochemical sources of acetone and methyl ethyl ketone along the back trajectory. Propane is estimated to contribute 50% of the acetone budget globally [*Singh et al.*, 1994], and methyl ethyl ketone is formed in the HO-initialized oxidation of butane in high yield [*Atkinson*, 1997]. Such production can markedly affect this estimation method of the A factor, the b factor, and HO, as it is essentially constrained by three parameters, the slope of the selected trace gases, and by the acetone and MEK loss rates. The net loss rate for these carbonyls is therefore the photolysis rate plus the loss by HO minus en route photochemical production rate. Hence HO will be underestimated. As the production of these carbonyl compounds along the back trajectory is dependent on the concentration of the precursor species, estimation of the contribution is difficult. CO can be similarly affected from CO produced through the oxidation of methane, but in this case the effect on the variability is less as the source is so homogeneous. Assuming photochemical production reduces the effective loss rate of acetone and MEK by half, then the resulting estimate for HO is 4.5×10^5 molecules cm^{-3}, chi squared 0.005. This HO value is still approximately a factor of 2 less than the model prediction. If we assume that the HO concentration is actually 1×10^6 molecules cm^{-3}, then the effective loss rate of acetone and MEK is approximately 4 times less than the calculated loss rate implying a significant production term. Acetone and MEK can be produced from the HO-initiated photochemical oxidation of the parent hydrocarbons propane and butane, respectively [*Atkinson*, 1997]. Moreover, there is evidence from field measurements of alkyl nitrates and hydrocarbons that acetone but not MEK is produced from the decomposition of larger organic compounds, specifically alkoxy radicals [*Bertman et al.*, 1995]. However, another possibility is that acetone and MEK could be directly emitted from the ocean along the back trajectory thus causing a lower effective loss rate to be observed for these compounds. Emission of carbonyls including acetone, resulting from photochemistry within the ocean surface, has been reported previously [*Zhou and Mopper*, 1997]. The size of the deduced production rate suggests that it will be of importance to the global budget of these compounds although the nature of the production cannot be attributed.

In this study so far we have considered only removal by HO and by photolysis. As the air masses measured have passed for several days over the ocean, we also consider the influence of halogen radicals on the variability curve. The presence of significant quantities of chlorine radicals would cause propane to lie outside the trend, as at 298 K the rate coefficients for the propane rate of reaction with Cl [*Tyndall et al.*, 1997] is almost 2 orders of magnitude larger than between propane and HO [*Donahue et al.*, 1998]. As first pointed out by *Jobson et al.* [1999, 1994], the presence of high concentrations of Br radicals can cause acetylene to lie outside the trend. The rate coefficient of acetylene with HO [*Bohn et al.*, 1996] is, however, approximately 1 order of magnitude larger than that of bromine [*Barnes et al.*, 1989], so very large concentrations of bromine would be required to compete with the HO reaction. The good fit to propane and acetylene obtained when using this derived HO concentration (see Plate 2b) suggests that significant removal of hydrocarbons by Cl and Br radicals does not occur in this region.

4. Discussion

The examination of Sigma_lnX versus lifetime has proven valuable in five important ways. It provides supporting evidence for the identification of masses in the PTR-MS. Second, it can help identify outliers in the hydrocarbon data set and

Table 3. Lists the Fit Parameters A and b to Sigma_ln(X) = $A\tau^{-b}$ for the LBA-CLAIRE Campaign, Two Previous Tropical Airborne Measurement Campaigns, and Harvard Forest

Campaign	A	b	Altitude of Data Used, km	Location	Time
LBA-Claire	4.63 ± 1.21	0.64 ± 0.07	0–1	1°–5.5°N, 54°–57°W Surinam	March
PEM-West B	4.3 ± 0.63[a]	0.53 ± 0.02	0–12	western Pacific	March
TRACE-A	2.9 ± 0.44[a]	0.52 ± 0.02	0–12	Brazil, southern Africa, South Atlantic	September
Harvard forest	0.99 ± 0.45[a]	0.18 ± 0.16	ground	northeast United States	Summer and winter

Further campaign information available for PEM-West B [*Hoell et al.*, 1997], TRAC-A [*Fishman et al.*, 1996], and Harvard forest [*Goldstein et al.*, 1996].

[a]From *Jobson et al.* [1999].

assess the quality of the measurements including data below detection limit (butane and pentane) as well as contamination and integration problems (toluene and ethane). It provides evidence of possible additional removal processes (acetonitrile) or halogen chemistry, and provides a formal method to analyze whether the atmospheric variability in a data set is greater than the instrumental precision. Finally, it may be used to estimate average HO concentrations that have been experienced along the back trajectory by air masses in the region investigated.

The coefficients A and b of the fit shown in Figure 4b can be compared with those from two other tropical data sets, Transport and Atmospheric Chemistry Near the Equator—Atlantic (Trace-A) and Pacific Exploratory Mission—West Phase B (PEM-West B), in Table 3. Trace-A took place in September 1992 over the South Atlantic, Brazil, and southern Africa, while PEM-West B took place between February and March 1994 over the western Pacific. The value of b found in this study is similar to but slightly higher than both other tropical data sets. The exponent b has been interpreted as a measure of the influence of mixing on the variability, where higher values signify the dominance of chemical loss processes. The data used by *Jobson et al.* [1999] to calculate b are solely canister data which cover a wide variety of altitudes. The lower values of b derived from this data suggest a stronger influence of mixing than for the LBA-CLAIRE data which was limited to the boundary layer, where relatively uniform northeasterly flow was experienced. The value of A presented here is in good agreement with that found from the PEM-West B data set but almost twice as large as that found in Trace-A (see Table 2). We interpret A as a measure of the range of air mass ages in the sampled data set, as determined by the time period between emission and measurement of the species in question. High values of A have been reported from the analysis of stratospheric data sets [*Jobson et al.*, 1999]. In the extreme case of the stratosphere we expect air masses directly mixed in from the troposphere and air masses several years old to be part of the analysis. The troposphere is generally better mixed than the stratosphere, but a range of air mass ages will be sampled, the size of which will depend on the time and location of the campaign. In the case of PEM-West B the coefficient A is also high which we interpret as an indication that this campaign measured air over the remote Pacific Ocean which was sufficiently aged so that contributions from all possible sources were encountered. The high values of A presented here from the LBA-CLAIRE campaign can similarly be understood in terms of a sampling of air transported over the unpolluted Atlantic Ocean. The low value of A reported for the Harvard forest site (see Table 2) we interpret as indicating that air masses with only a small range of ages were sampled, in this case only relatively fresh continental emissions. For the Harvard forest site the coefficient b, the measure of the effect of chemistry on the sample, is low: 0.18 ± 0.16 [*Jobson et al.*, 1999]. Similarly, there is little observable trend ($b \approx 0$) in the present isoprene, MVK/MACR, and hydroxyacetone data, which are a biogenic emission, a first-order, and second-order photoproduct, respectively (see Figure 2).

The lower A value for the TRACE-A study is more difficult to understand, but may be associated with a distribution of travel times (or sources) which is skewed toward nearby continental sources in Brazil or in South Africa during the biomass burning season. These sources of NMHC are not operative in our measurement region, and the LBA-CLAIRE data are therefore more similar to PEM-West B.

Development of such semiempirical models lead to a better understanding of how and to what extent variability can be related to atmospheric processes. Considered in this study is variability caused by instrumental noise, variability in the source emission rate, variability in proximity to sources, and by chemical loss process and transport. In the simple model of variability presented here, where a nominal instrument precision of 1% is chosen, the distance along the back trajectory which generates variability is estimated to approximately 4–5 lifetimes of the species multiplied by the wind speed. The fetch contributing to the variability of a species is determined by its lifetime. With isoprene, MVK/MACR, and hydroxyacetone we exemplify how local highly varying sources of a species can overwhelm the variability induced through chemical loss mechanisms. We also show that for species with distant sources that a trend can be found in data, measured by three different instruments, which relates to the chemical and dynamical history of the air parcel. This trend has been exploited to aid identification of PTR-MS masses and to derive HO concentrations semiempirically as discussed below.

Presented here is a new indirect method of estimating the average HO concentrations experienced by an air mass along its back trajectory. The hydroxyl radical plays a critical role in the chemistry of the lower atmosphere, and an understanding

of its production, interconversion, and sinks is central to modeling and predicting the chemistry of the troposphere. Concentrations of HO are small, and hence direct measurement is complicated. In the future, by this method, experimentalists could empirically calculate average HO values along a back trajectory to a source, provided that large measurement sets of selected compounds are made and photolysis rates are known. The technique, however, has limitations. The calculated HO is suppressed by the presence of photochemical sources of acetone and MEK. In areas where strong point sources exist, no dependency between variability and lifetime can be expected [*Jobson et al.*, 1998], and hence this treatment cannot be performed as the variability is no longer being controlled by removal processes. Similarly, limitations of this method can be expected for species which can be affected by halogen chemistry. However, for remote sites or for those with homogeneous sources, large measurement data sets including species that have a photolysis component can be used to derive the historical average HO concentration since source. The tropics are ideal areas for such measurements as the meteorology is similar from one day to the next ensuring the photolysis component of the lifetimes does not fluctuate greatly. Long-term measurements of selected compounds at such sites could potentially be used to track the seasonal change in the HO concentrations, using this technique.

Acknowledgments. The authors thank the staff of the Delft University of Technology, the pilots, engineers, and crew of the Citation, and the staff of the Surinam Meteorological Service for their able assistance and professionalism. We thank the two anonymous reviewers for their comments and Tom Jobson for helpful discussions. The support of the Max Planck Gesellschaft, the Austrian Academy of Sciences, the DDG, and the international research school COACh is gratefully acknowledged.

References

Anderson, L. G., L. S. Baily, and J. A. Lanning, Spatial and temporal variability of carbonyl compounds in the Denver metropolitan area, paper presented at 89th Annual Meeting, Air and Waste Manage. Assoc., Nashville, Tenn., 1996.

Andreae, M. O., R. W. Talbot, T. W. Andreae, and R. C. Harriss, Formic and acetic acid over the central Amazon region, Brazil, 1, Dry season, *J. Geophys. Res.*, *93*, 1616–1624, 1988.

Atkinson, R., Kinetics and mechanisms of the gas-phase reactions of the hydroxyl radical with organic compounds, *J. Phys. Chem. Ref. Data Monogr.*, *1*, 121–126, 1989.

Atkinson, R., Gas-phase tropospheric chemistry of organic compounds, *J. Phys. Chem. Ref. Data*, *26*, 215–290, 1997.

Atkinson, R., D. L. Baulch, R. A. Cox, R. F. Hampson, J. A. Kerr, M. J. Rossi, and J. Troe, Evaluated kinetic and photochemical data for atmospheric chemistry, supplement VI, IUPAC Subcommittee on Gas Kinetic Data Evaluation for Atmospheric Chemistry, *J. Phys. Chem. Ref. Data*, *26*, 1329–1499, 1997.

Barnes, I., V. Bastian, K. H. Becker, R. Overath, and Z. Tong, Rate constants for the reactions of Br atoms with a series of alkanes, alkenes, and alkynes in the presence of O_2, *Int. J. Chem. Kinet.*, *21*, 499–517, 1989.

Baulch, D. L., R. A. Cox, P. J. Crutzen, R. F. Hampson Jr., J. A. Kerr, J. Troe, and R. T. Watson, Evaluated kinetic and photochemical data for atmospheric chemistry, supplement I, CODATA task group on chemical kinetics, *J. Phys. Chem. Ref. Data*, *11*, 327–496, 1982.

Benkelberg, H.-J., S. Hamm, and P. Warneck, Henry's law coefficients for aqueous solutions of acetone, acetaldehyde and acetonitrile and equilibrium constants for the addition of acetone and acetaldehyde with bisulphate, *J. Atmos. Chem.*, *20*, 17–34, 1995.

Bertman, S. B., J. M. Roberts, D. D. Parrish, M. P. Buhr, P. D. Goldan, W. C. Kuster, F. C. Fehsenfeld, S. A. Monska, and H. Westberg, Evolution of alkyl nitrates with air mass age, *J. Geophys. Res.*, *100*, 22,805–22,813, 1995.

Bohn, B., M. Siese, and C. Zetzsch, Kinetics of the OH + C_2H_2 reaction in the presence of O_2, *J. Chem. Soc. Faraday Trans.*, *92*, 1459–1466, 1996.

Brühl, C., and P. J. Crutzen, On the disproportionate role of tropospheric ozone as a filter against solar UV-B radiation, *Geophys. Res. Lett.*, *16*, 703–706, 1989.

Crutzen, P. J., A. C. Delany, J. P. Greenberg, P. Haagenson, L. Heidt, R. Luer, W. Pollock, W. Seiler, A. Wartburg, and P. R. Zimmerman, Tropospheric chemical composition mearsurements in Brazil during the dry season, *J. Atmos. Chem.*, *2*, 233–256, 1985.

de Gouw, J. A., C. J. Howard, T. G. Custer, and R. Fall, Emission of volatile organic compounds from cut grass and clover are enhanced during the drying process, *Geophys. Res. Lett.*, *26*, 811–814, 1999.

Demore, W. B., S. P. Sander, C. J. Howard, A. R. Ravishankara, D. M. Golden, C. E. Kolb, R. F. Hampson, M. J. Kurylo, and M. J. Molina, Chemical kinetics and photochemical data for use in stratospheric modeling, *JPL Publ.*, *97-4*, 1997.

Donahue, N. M., J. G. Anderson, and K. L. Demerjian, New rate constants for ten OH alkane reactions from 300 to 400 K: An assessment of accuracy, *J. Phys. Chem. A*, *102*, 3121–3126, 1998.

Ehhalt, D. H., F. Rohrer, A. Wahner, M. J. Prather, and D. Blake, On the use of hydrocarbons for the determination of tropospheric OH concentrations, *J. Geophys. Res.*, *103*, 18,981–18,997, 1998.

Fishman, J., J. M. Hoell, R. D. Bendura, R. J. McNeil, and V. Kirchhoff, NASA GTE TRACE-A experiment (September–October 1992): Overview, *J. Geophys. Res.*, *101*, 23,865–23,879, 1996.

Gierczak, T., J. B. Burkholder, R. K. Talukdar, A. Mellouki, S. B. Barone, and A. R. Ravishankara, Atmospheric fate of methyl vinyl ketone and methacrolein, *J. Photochem. Photobiol. A Chem.*, *110*, 1–10, 1997.

Goldstein, A. H., S. M. Fan, M. L. Goulden, J. W. Munger, and S. C. Wofsy, Emissions of ethene, propene, and 1-butene by a midlatitude forest, *J. Geophys. Res.*, *101*, 9149–9157, 1996.

Hamm, S., J. Hahn, G. Helas, and P. Warneck, Acetonitrile in the troposphere: Residence time due to rainout and uptake by ocean, *Geophys. Res. Lett.*, *11*, 1207–1210, 1984.

Hamrud, M., Residence time and spatial variability for gases in the atmosphere, *Tellus, Ser. B*, *35*, 293–303, 1983.

Hansel, A., A. Jordan, R. Holzinger, P. Prazeller, W. Vogel, and W. Lindinger, Proton transfer reaction mass spectrometry on-line trace gas analysis at the ppb level, *Int. J. Mass Spectrom. Ion Processes*, *149*, 609–619, 1995.

Heiden, A. C., K. Kobel, M. Komenda, R. Koppman, M. Shao, and J. Wildt, Toluene emission from plants, *Geophys. Res. Lett.*, *26*, 1283–1286, 1999.

Hoell, J. M., D. D. Davis, S. C. Liu, R. E. Newell, H. Akimoto, R. J. Mcneal, and R. J. Bendura, Pacific Exploratory Mission-West Phase B: February–March 1994, *J. Geophys. Res.*, *102*, 28,223–28,239, 1997.

Holzinger, R., C. Warneke, A. Hansel, A. Jordan, W. Lindinger, D. H. Scharffe, G. Schade, and P. J. Crutzen, Biomass burning as a source of formaldehyde, acetaldehyde, methanol, acetone, acetonitrile, and hydrogen cyanide, *Geophys. Res. Lett.*, *26*, 1161–1164, 1999.

Jenkin, M. E., S. M. Saunders, and M. J. Pilling, The tropospheric degradation of volatile organic compounds: A protocol for mechanism development, *Atmos. Environ.*, *31*, 81–104, 1997.

Jobson, B. T., H. Niki, Y. Yokouchi, J. Bottenheim, F. Hopper, and R. Leaitch, Measurements of C_2-C_6 hydrocarbons during the Polar Sunrise 1992 Experiment: Evidence for Cl atom and Br atom chemistry, *J. Geophys. Res.*, *99*, 25,355–25,368, 1994.

Jobson, B. T., D. D. Parrish, P. Goldan, W. Kuster, F. C. Fehsenfeld, D. R. Blake, N. J. Blake, and H. Niki, Spatial and temporal variability of nonmethane hydrocarbon mixing ratios and their relation to photochemical lifetime, *J. Geophys. Res.*, *103*, 13,557–13,567, 1998.

Jobson, B. T., S. A. McKeen, D. D. Parrish, F. C. Fehsenfeld, D. R. Blake, A. H. Goldstein, S. M. Schauffler, and J. W. Elkins, Trace gas mixing ratio variability versus lifetime in the troposphere and stratosphere: Observations, *J. Geophys. Res.*, *104*, 16.090–16,113, 1999.

Jordan, A., R. Holzinger, and W. Lindinger, Acetonitrile and benzene in the breath of smokers and non-smokers investigated by proton transfer mass spectrometry (PTR-MS), *Int. J. Mass Spectom. Ion Processes*, *148*, L1–L3, 1995.

Junge, C. E., Residence time and variability of tropospheric trace gases, *Tellus*, *16*, 477–488, 1974.

Kesselmeier, J., and M. Staudt, Biogenic volatile organic compounds

(VOC): An overview on emission, physiology and ecology, *J. Atmos. Chem.*, *33*, 23–38, 1999.

Kirstine, W., I. Galbally, Y. R. Ye, and M. Hooper, Emissions of volatile organic compounds (primarily oxygenated species) from pasture, *J. Geophys. Res.*, *103*, 10,605–10,619, 1998.

Kuhlman, R. V., M. Lawrence, U. Pöschl, and P. J. Crutzen, Sensitivity studies of isoprene and acetone chemistry in a 3D global model, in *EGS*, edited by A. K. Richter, 498 pp., Eur. Geophys. Soc., The Hague, 1999.

Lawrence, M., P. J. Crutzen, P. Rasch, B. E. Eaton, and N. Mahowald, A model for studies of tropospheric photochemistry: Description, global distributions, and evaluation, *J. Geophys. Res.*, *104*, 26,245–26,277, 1999.

Le Calve, S., D. Hitier, G. Lebras, and A. Mellouki, Kinetic studies of OH reactions with a series of ketones, *J. Phys. Chem.*, *102*, 4579–4584, 1998.

Lelieveld, J., A. Bregman, H. A. Scheeren, J. Ström, K. Carslaw, H. Fischer, P. C. Siegmund, and F. Arnold, Chlorine activation and ozone destruction in the northern lowermost stratosphere, *J. Geophys. Res.*, *104*, 8201–8214, 1999.

Lindinger, W., and A. Hansel, Analysis of trace gases at ppb levels by proton transfer reaction mass spectrometry (PTR-MS), *Plenum Sources Sci. Technol.*, *6*, 1–7, 1997.

Lindinger, W., A. Hansel, and A. Jordan, On-line monitoring of volatile organic compounds at pptv levels by means of proton transfer mass spectrometry (PTR-MS)—Medical applications, food control and environmental research [review], *Int. J. Mass Spectrom. Ion Processes*, *173*, 191–241, 1998.

O'Brien, J. M., P. B. Shepson, Q. Wu, T. Biesenthal, J. W. Bottenheim, H. A. Wiebe, K. G. Anlauf, and P. Brickell, Production and distribution of organic nitrates, and their relationship to carbonyl compounds in an urban environment, *Atmos. Environ.*, *31*, 2059–2069, 1997.

Pöschl, U., et al., High acetone concentrations throughout the troposphere over the tropical rainforest in Surinam, *J. Atmos. Chem.*, in press, 2000.

Schneider, J., V. Burger, and F. Arnold, Methyl cyanide and hydrogen cyanide measurements in the lower stratosphere: Implications for methyl cyanide sources and sinks, *J. Geophys. Res.*, *102*, 25,501–25,506, 1997.

Singh, H. B., D. O'Hara, D. Herlth, W. Sachse, D. R. Blake, J. D. Bradshaw, M. Kanakidou, and P. J. Crutzen, Acetone in the atmosphere: Distribution, sources, and sinks, *J. Geophys. Res.*, *99*, 1805–1819, 1994.

Taucher, J. A., A. Hansel, A. Jordan, and W. Lindinger, Analysis of compounds in human breath after ingestion of garlic using proton-transfer reaction mass spectrometry, *J. Agric. Food Chem.*, *44*, 3778–3782, 1996.

Tuazon, E. C., and R. Atkinson, A product study of the gas-phase reaction of isoprene with the OH radical in the presence of NO_x, *Int. J. Chem. Kinet.*, *22*, 1221–1236, 1990.

Turnipseed, A. A., S. B. Barone, and A. R. Ravishankara, Reaction of OH with dimethyl sulfide, 2, Products and mechanisms, *J. Phys. Chem.*, *100*, 14,703–14,713, 1996.

Tyndall, G. S., J. J. Orlando, T. J. Wallington, M. Dill, and E. W. Kaiser, Kinetics and mechanisms of the reactions of chlorine atoms with ethane, propane, and n-butane, *Int. J. Chem. Kinet.*, *29*, 43–55, 1997.

Warneke, C., J. Kuczynski, A. Hansel, A. Jordan, W. Vogel, and W. Lindinger, Proton transfer reaction mass spectrometry (PTR-MS): Propanol in human breath, *Int. J. Mass Spectrom. Ion Processes*, *154*, 61–70, 1996.

Warneke, C., T. Karl, H. Judmaier, A. Hansel, A. Jordan, W. Lindinger, and P. Crutzen, Acetone, methanol, and other partially oxidized volatile organic emissions from dead plant matter by abiological processes: Significance for atmospheric chemistry, *Global Biogeochem. Cycles*, *13*, 9–18, 1999.

Warneke, C., et al., Isoprene and its oxidation products methyl vinyl ketone, methacrolein and isoprene peroxides measured online over a tropical rainforest during the LBA-CLAIRE campaign in Surinam 1998, *J. Atmos. Chem.*, in press, 2000.

Wideqvist, S., The alkaline hydrolysis of acetonitrile, *Ark. Kemi.*, *10*, 265–270, 1956.

Wienhold, F. G., et al., TRISTAR—A tracer in situ TDLAS for atmospheric research, *Appl. Phys. B*, 411–417, 1998.

Williams, J., U. Pöschl, P. J. Crutzen, A. Hansel, R. Holzinger, C. Warneke, W. Lindinger, and J. Lelieveld, An atmospheric chemistry interpretation of mass scans obtained from a proton transfer mass spectrometer flown over the tropical rain forest of Surinam, *J. Atmos. Chem.*, in press, 2000.

Zhou, X., and K. Mopper, Photochemical production of low molecular weight carbonyl compounds in seawater and surface microlayer and their air-sea exchange, *Mar. Chem.*, *56*, 201–213, 1997.

P. J. Crutzen, H. Fischer, R. Holzinger, P. Hoor, and J. Williams, Max Planck Institute for Chemistry, Mainz D-55128, Germany. (williams@mpch-mainz.mpg.de)

A. Hansel and W. Lindinger, Institute for Ionphysics, Innsbruck University, A-6020 Innsbruck, Austria.

G. W. Harris, Centre for Atmospheric Chemistry, York University, Toronto, Ontario, Canada M3J 1P3.

J. Lelieveld, B. Scheeren, and C. Warneke, Institute for Marine and Atmospheric Research, Utrecht University, Utrecht 3584 CC, Netherlands.

(Received November 10, 1999; revised March 24, 2000; accepted March 28, 2000.)